World Journal of Radiology

Submit a Manuscript: https://www.f6publishing.com

World J Radiol 2024 December 28; 16(12): 749-759

DOI: 10.4329/wjr.v16.i12.749

ISSN 1949-8470 (online)

ORIGINAL ARTICLE

Retrospective Cohort Study

Normative vertebral deformity measurements in a clinically relevant population using magnetic resonance imaging

Olivia R Sorci, Rashad Madi, Sun Min Kim, Alexandra S Batzdorf, Austin Alecxih, Julia N Hornyak, Sheenali Patel, Chamith S Rajapakse

Specialty type: Radiology, nuclear medicine and medical imaging

Provenance and peer review: Invited article; Externally peer reviewed.

Peer-review model: Single blind

Peer-review report's classification

Scientific Quality: Grade B, Grade B, Grade B

Novelty: Grade A, Grade B, Grade C

Creativity or Innovation: Grade A, Grade B, Grade C

Scientific Significance: Grade B, Grade B, Grade B

P-Reviewer: Shi K; Zhu BT

Received: March 28, 2024

Revised: October 15, 2024

Accepted: December 12, 2024

Published online: December 28, 2024

Processing time: 273 Days and 12.2 Hours

Olivia R Sorci, Rashad Madi, Sun Min Kim, Alexandra S Batzdorf, Austin Alecxih, Julia N Hornyak, Sheenali Patel, Chamith S Rajapakse, Department of Radiology, University of Pennsylvania, Philadelphia, PA 19104, United States

Corresponding author: Rashad Madi, MD, Postdoctoral Fellow, Department of Radiology, University of Pennsylvania, 3450 Hamilton Walk, Philadelphia, PA 19104, United States. rashad.madi@pennmedicine.upenn.edu

Abstract

BACKGROUND

Osteoporosis is the leading cause of vertebral fractures. Dual-energy X-ray absorptiometry (DXA) and radiographs are traditionally used to detect osteoporosis and vertebral fractures/deformities. Magnetic resonance imaging (MRI) can be utilized to detect the relative severity of vertebral deformities using three-dimensional information not available in traditional DXA and lateral two-dimensional radiography imaging techniques.

AIM

To generate normative vertebral parameters in women using MRI and DXA scans, determine the correlations between MRI-calculated vertebral deformities and age, DXA T-scores, and DXA Z-scores, and compare MRI vertebral deformity values with radiography values previously published in the literature.

METHODS

This study is a retrospective vertebral morphometric analysis conducted at our institution. The patient sample included MR images from 1638 female patients who underwent both MR and DXA imaging between 2005 and 2014. Biconcavity, wedge, crush, anterior height (H_a)/posterior height (Hp), and middle height (H_m)/posterior height values were calculated from the MR images of the patient's vertebrae. Associations between vertebral deformity values, patient age, and DXA T-scores were analyzed using Spearman correlation. The MRI-derived measurements were compared with radiograph-based calculations from population-based data compiled from multiple studies.

RESULTS

Age was positively correlated with lumbar H_m/H_p (P = 0.04) and thoracic wedge

(P = 0.03) and biconcavity (P = 0.001) and negatively correlated with thoracic H_a/H_p (P = 0.002) and H_m/H_p (P = 0.001) values. DXA T-scores correlated positively with lumbar H_m/H_p (P < 0.0001) and negatively with lumbar wedge (P = 0.046), biconcavity (P < 0.0001), and H_a/H_p (P = 0.046) values. Qualitative analysis revealed that H_a/H_p differed between MRI and radiography population-based data by no more than 0.3 and H_m/H_p by a maximum of 1.2.

CONCLUSION
Compared with traditional imaging techniques, MRI detects vertebral deformities with high accuracy and reliability. It may be a sensitive, ionizing, radiation-free tool for use in clinical settings.

Key Words: Magnetic resonance imaging; Dual-energy X-ray absorptiometry; Radiography; Vertebral deformities; Biconcavity; Wedge; Crush; Vertebral fractures

Core Tip: This study provides new reference data for vertebral deformities using Magnetic Resonance Imaging (MRI) to assess vertebral heights and deformities in women. We correlated MRI-derived measurements with age and dual-energy X-ray absorptiometry scores, revealing key insights into the progression of spinal deformities. Our results highlight the potential of MRI to accurately measure vertebral deformities, offering improved diagnostic capabilities and a non-invasive approach for monitoring spinal health.

Citation: Sorci OR, Madi R, Kim SM, Batzdorf AS, Alecxih A, Hornyak JN, Patel S, Rajapakse CS. Normative vertebral deformity measurements in a clinically relevant population using magnetic resonance imaging. *World J Radiol* 2024; 16(12): 749-759
URL: https://www.wjgnet.com/1949-8470/full/v16/i12/749.htm
DOI: https://dx.doi.org/10.4329/wjr.v16.i12.749

INTRODUCTION

Osteoporosis is a skeletal disorder characterized by low bone mass and microarchitectural deterioration, leading to bone fragility and increased risk of fractures. As human life expectancy increased, osteoporosis became the leading bone disease in prevalence and economic cost[1]. Vertebral fractures are the most common manifestation of osteoporosis, comprising almost 50% of all osteoporotic fractures in the United States annually, leading to a significant burden on our healthcare system[2]. Patients have an increased medical cost of $38649 in their first year after an osteoporotic vertebral fracture compared to their healthy-matched counterparts[3]. Moreover, vertebral fractures have been linked to physical disabilities, reduced mobility, increased anxiety and depression, and increased mortality[4-6]. They frequently occur in the elderly population, particularly postmenopausal women, due to decreased estrogen production, eventually resulting in osteoporosis[7]. Furthermore, a single vertebral fracture substantially increases the risk of subsequent osteoporotic fractures, both vertebral and non-vertebral. Osteoporotic vertebral fractures cause a wide range of symptoms depending on the location and severity, meaning no stereotypical symptoms are associated with these fractures. They, therefore, tend to be underdiagnosed and missed by clinicians. Only one-third of vertebral fractures are clinically diagnosed, resulting in unnecessary long-term pain and the accumulation of severe spinal deformities over time[4].

There are several methods to detect vertebral fractures. However, the variation in shape and size of the vertebrae individually and between patients leads to great uncertainty in the diagnosis. In qualitative visual diagnoses, the assessment of vertebral fractures is primarily determined by individual clinicians' interpretations of radiographic appearances. Dual-energy X-ray absorptiometry (DXA) scans have been the gold standard in diagnosing osteoporosis, while vertebral compression fractures are diagnosed using lateral X-ray imaging of the spine[8]. DXA scans accurately measure bone mineral density (BMD) and can provide a clear lateral image of the lower thoracic and lumbar spine. This method allows for simultaneous assessment of overall bone quality and vertebral fracture status[9]. DXA scans use a low dose of ionizing radiation, require minimal patient setup, and have a short scan time[10], but they do not provide a clear image of the upper thoracic vertebrae[11].

Lateral plain X-ray radiographs use the Genant semi-quantitative approach, which reduces the subjectivity of a vertebral fracture assessment. This approach utilizes a visual grading scale to categorize the severity of vertebral deformities. Each vertebra's severity grade is assigned based on the visually apparent degree of vertebral height loss. Vertebral fractures are classified as grade 1 if the vertebral height is reduced by 20%-25%, grade 2 if reduced by 25%-40%, or grade 3 if reduced by 40% or more[12]. Large amounts of bone loss, typically 40%-50%, are required before abnormalities on lateral radiographs can be detected easily[13]. Vertebral fractures may be quantified by setting a fracture threshold based on the average vertebral deformity of a reference population, as proposed by Eastell *et al*[14], Rajapakse *et al*[15] and Jiang *et al*[16]. Vertebral deformities can be characterized as wedge, biconcavity, or crush, depending on the anterior (H_a), middle (H_m), and posterior (H_p) heights of each vertebral body[12]. A wedge deformity is defined as an anterior-posterior asymmetry. Biconcavity deformities are characterized by decreased H_m relative to H_p. Crush deformi-

ties are described as vertebral compression relative to neighboring vertebrae. Wedge, biconcavity, and crush deformities comprise 50%, 17%, and 13% of prevalent fractures among adults, respectively[15].

Each vertebra is a three-dimensional entity. Hence, two-dimensional (2D) imaging may not be the most accurate method to analyze vertebral fractures, especially since the spine is inherently curved. The spinal curvature must be assessed to evaluate a spinal deformity accurately. 2D imaging only depicts the spinal anatomy from a single plane, meaning an exact description of the spinal curvature cannot be fully determined from 2D imaging alone[17]. Thus, the multi-slice magnetic resonance imaging (MRI)-based approach developed by Rajapakse *et al*[15] is a promising tool for measuring the relative severity of spinal deformities accurately and reliably. The MRI-based approach provides improved spatial resolution with good signal, contrast properties, and multiplanar reconstruction[18,19].

This study utilized MR images to establish new reference data for vertebral wedge, biconcavity, and crush deformities for vertebrae C3 through L5 in females. We sought to validate this data by comparing it to previously published 2D-derived vertebral heights and correlating the deformity severity with age and DXA T- and Z-scores. Standard deformity curves at each vertebral level would allow clinicians to accurately determine the relative severity of spinal deformities.

MATERIALS AND METHODS

This was a retrospective vertebral morphometric study with both between-participant and within-participant components. The institutional review board approved the procedures, and written informed consent was obtained from all participants.

MRI cohort

Analyses were conducted using multi-slice spine MR images from 1638 female patients who underwent both MR and DXA imaging at our institution between January 1, 2005 and January 20, 2014. Due to the severe nature of osteoporosis among women, we excluded male participants from this study. To maximize the sample size and capture the diversity of individuals obtaining spinal DXA and MR images, the exclusion criteria did not include any specific blood chemistry values or other clinical diagnoses. Female participants (n = 1638) with a mean ± SD age of 67.6 ± 10.9 years (range: 27-98 years) were included in this study.

Spine MRI acquisition

Vertebral deformity analyses were performed on sagittal images of the vertebral spine (Figure 1). These were acquired using a fast spin-echo sequence: Magnetic field strength, 1.5-3 T; slice thickness, 3-4 mm; repetition time, mean = 625.77 ms, range 250-5000 ms; echo time, mean = 11.86 ms, range 5.56-101.02 ms; voxel size, mean = 0.55 mm, range 0.25-1.5 mm; and matrix size, mean = 487.56 mm, range 256-1024 mm.

DXA-derived BMD T-score and Z-score

BMD scores were obtained from DXA scans conducted for various clinical workups. T-scores are reported as a reference for diagnosing osteopenia and osteoporosis, along with other associations calculated between DXA BMD scores and deformity values.

Vertebral deformity quantification

Deformities were quantified using software written in Interactive Data Language (Exelis Visual Information Solutions, Inc., Boulder, Colorado) described previously by Rajapakse *et al*[15]. A stack of sagittal images was displayed, the image crossing each vertebra in the midline was located, and the four corners and superior and inferior midline edges were annotated manually. Special precautions were taken to avoid errors due to osteophytes and depressions caused by endplate herniations (Schmorl's nodes). Euclidean distances between annotations were used to calculate the H_a/H_p and H_m/H_p ratios and wedge, biconcavity, and crush deformities using the formulas (Table 1). The number of vertebrae analyzed per participant varied based on height due to a fixed field of view and the visualization of individual vertebrae on MR images.

2D radiography existing literature

We focused on gathering literature that utilizes radiographs to calculate spinal deformities[20-30]. The main objectives of the studies we collected to calculate spinal deformities in radiographs were to establish vertebral spinal deformity reference values dependent on population-based data. Eleven studies were examined initially, with sample sizes large enough that the vertebral values calculated in each study were deemed representative of the values likely to occur in the participants' demographics[20-30]. Studies were excluded if vertebral calculations did not include enough spine segments. For example, radiography is often limited in the thoracic spine due to its low image quality. In total, the average age of participants in the 2D imaging studies was 63.5 years.

Statistical analysis

Statistical significance was set at $\alpha = 0.05$. All analyses were performed using R (version 3.5.1, R Foundation for Statistical Computing, Vienna, Austria). Within the MR imaging cohort, DXA T-score and Z-score, as well as corresponding healthy, osteopenia, or osteoporosis designations, were previously determined clinically. For each deformity type, Spearman's rank correlation coefficient was calculated to investigate the association between lumbar deformity severity and DXA-

Table 1 Vertebral deformity formulas

	Cervical vertebrae	Thoracic vertebrae	Lumbar vertebrae
Wedge	$1 - H_p/H_a$	$H_p/H_a - 1$	$1 - H_p/H_a$
Biconcavity	$H_a/H_m - 1$	$H_p/H_m - 1$	$H_a/H_m - 1$
Crush	$([H]_{above} + [H]_{below})/2[H] - 1$	$([H]_{above} + [H]_{below})/2[H] - 1$	$([H]_{above} + [H]_{below})/2[H] - 1$

[H]: $(H_a + H_m + H_p)/3$; H_a: Anterior height; H_m: Middle height; H_p: Posterior height.

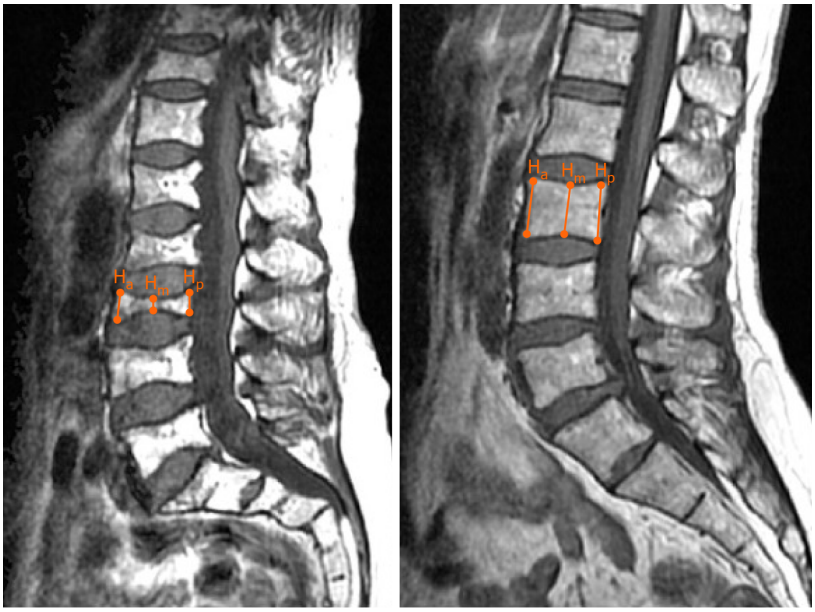

Figure 1 Representative magnetic resonance imaging demonstrating a severe L2 biconcavity deformity (left) and no L2 deformity (right) with anterior, middle, and posterior height measurements. H_a: Anterior height; H_m: Middle height; H_p: Posterior height.

derived T-score and Z-score.

Each deformity value and height ratio were averaged within vertebral regions to generate severity measures for the cervical, thoracic, and lumbar spine. Spearman's correlations were conducted to determine associations between age and the deformity values of each vertebral region (cervical, thoracic, and lumbar). The between-participant component involved plotting the MR imaging cohort's vertebral height values against those collected from the literature. The mean height values (H_a/H_p and H_m/H_p) were calculated for individual vertebrae (T1-L5) in each study. C3-C7 vertebrae were excluded from these analyses as images did not permit an accurate and complete assessment of these vertebrae.

RESULTS

Individual vertebral measurements

Deformities (wedge, crush, and biconcavity) and height ratios (H_a/H_p and H_m/H_p) were calculated for each vertebra (C3-L5) for 1638 female participants. Wedge, crush, and biconcavity deformity values are shown (Figure 2A). The mean ± SD values of the wedge deformities of the cervical, thoracic, and lumbar regions are -2.99 ± 2.45, 8.40 ± 3.41, and 3.60 ± 7.43, respectively. The mean ± SD of the crush deformities of the cervical, thoracic, and lumbar regions are 1.62 ± 3.68, -0.52 ± 1.07, and 0.41 ± 2.00, respectively. The mean ± SD of the biconcavity deformities of the cervical, thoracic, and lumbar regions are 11.43 ± 3.83, 12.41 ± 7.20, and 13.30 ± 4.25, respectively.

H_a/H_p and H_m/H_p values are shown in Figure 2B. The mean ± SD H_a/H_p ratios of the cervical, thoracic, and lumbar regions are 0.97 ± 0.02, 0.93 ± 0.03, and 1.04 ± 0.07, respectively. The mean ± SD H_m/H_p ratios of the cervical, thoracic, and lumbar regions are 0.88 ± 0.02, 0.88 ± 0.01, and 0.92 ± 0.03, respectively. The deformity values of each vertebra are presented in Table 2.

Relationship with age

Table 3 contains correlations between age and vertebral deformity values. Age was positively correlated with thoracic wedge (r_s = 0.06, P = 0.03) and biconcavity deformity values (r_s = 0.09, P = 0.001) (Figure 3A) and negatively correlated

Table 2 Reference spinal deformities of individual cervical, thoracic, and lumbar vertebrae in women (*n* = 1638)

Vertebra	Wedge	Crush	Biconcavity	H_a/H_p	H_m/H_p
C3	-1.66	-4.12	15.61	0.98	0.86
C4	-1.54	0.26	15.31	0.98	0.87
C5	-7.21	1.85	7.32	0.93	0.87
C6	-4.17	7.19	7.62	0.96	0.90
C7	-0.36	2.92	12.27	1.00	0.90
Total cervical, mean ± SD	-2.99 ± 2.45	1.62 ± 3.68	11.43 ± 3.83	0.97 ± 0.02	0.88 ± 0.02
T1	4.38	2.91	10.19	0.96	0.91
T2	1.85	-1.87	10.17	0.98	0.91
T3	4.50	-1.61	11.68	0.96	0.89
T4	8.43	-0.36	12.22	0.93	0.89
T5	10.06	-0.17	12.45	0.91	0.88
T6	13.94	0.70	16.08	0.88	0.86
T7	11.60	0.29	15.41	0.90	0.87
T8	12.01	-0.028	14.35	0.90	0.88
T9	9.84	1.20	14.4	0.93	0.88
T10	6.95	-0.05	14.47	0.94	0.88
T11	10.13	0.07	14.64	0.91	0.87
T12	7.17	-0.84	12.46	0.93	0.89
Total thoracic, mean ± SD	8.40 ± 3.41	-0.52 ± 1.07	13.38 ± 1.89	0.93 ± 0.03	0.88 ± 0.01
L1	-5.22	-1.44	7.09	0.95	0.89
L2	-1.84	-1.02	10.94	0.98	0.89
L3	2.30	-1.21	13.84	1.02	0.90
L4	6.64	-1.94	14.71	1.07	0.94
L5	16.16	3.54	19.93	1.16	0.97
Total lumbar, mean ± SD	3.61 ± 7.43	-0.41 ± 2.00	13.3 ± 4.25	1.04 ± 0.07	0.92 ± 0.03

H_a: Anterior height; H_m: Middle height; H_p: Posterior height.

Table 3 Deformity values of cervical, thoracic, and lumbar vertebral regions correlated with age, *P* value

	Wedge	Crush	Biconcavity	H_a/H_p	H_m/H_p
Cervical	0.41	0.29	0.88	0.41	0.87
Thoracic	0.03	0.18	0.001	0.002	0.001
Lumbar	0.61	0.85	0.33	0.61	0.04

H_a: Anterior height; H_m: Middle height; H_p: Posterior height.

with thoracic H_a/H_p (r_s = -0.08, P = 0.002) and H_m/H_p (r_s = -0.09, P = 0.001) (Figure 3B). Also, age was positively correlated with lumbar H_m/H_p (r_s = 0.06, P = 0.04) (Figure 3C).

BMD scores

Clinically calculated DXA T- and Z-scores for the MRI cohort are reported (Table 4). Based on their T-scores, 61.76% of the cohort had osteoporosis, 29.37% had osteopenia, and 8.87% had normal bone density. DXA T-scores were negatively correlated with lumbar wedge (r_s = -0.24, P < 0.0001) and biconcavity (r_s = -0.06, P = 0.046) (Figure 4A). They were also negatively correlated with H_a/H_p (r_s = -0.06, P = 0.046), but positively correlated with H_m/H_p (r_s = 0.17, P < 0.0001)

Table 4 Dual-energy X-ray absorptiometry T-score and Z-score of the magnetic resonance imaging cohort (*n* = 1638)

	mean ± SD	Median ± IQR	Range
T-score	-0.3 ± 1.82	-0.5 ± 1.15	-7.4-8.0
Z-score	0.8 ± 1.77	-0.7 ± 1.10	-5.3-9.0

IQR: Interquartile range.

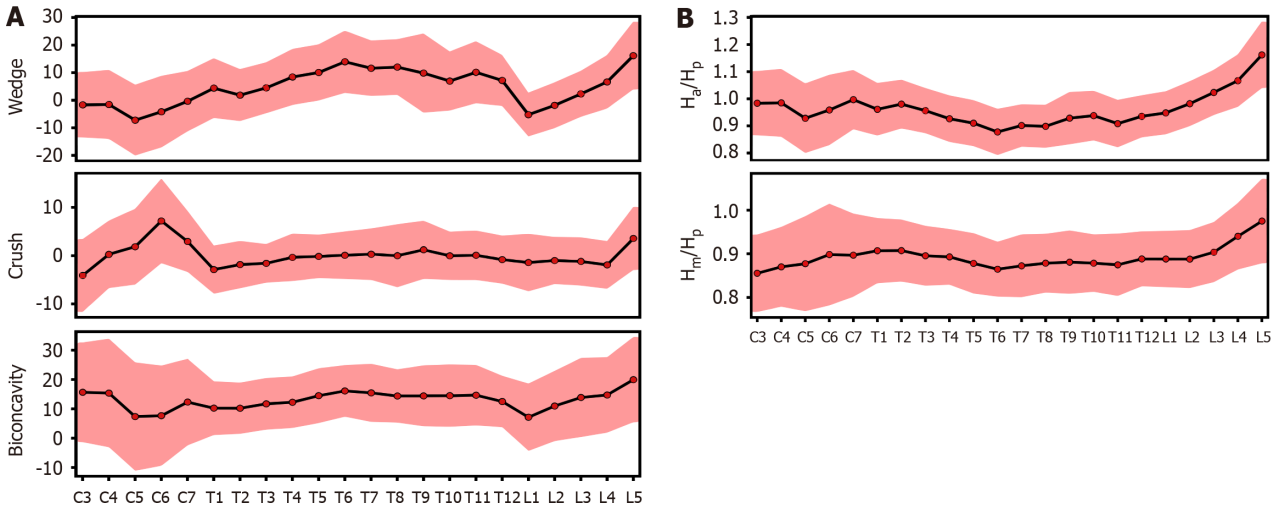

Figure 2 Individual vertebral measurements. A: Mean wedge, crush, and biconcavity deformities of vertebrae C3-L5; B: Mean anterior height/posterior height and middle height/posterior height ratios of vertebrae C3-L5. Error clouds represent SD. H_a: Anterior height; H_m: Middle height; H_p: Posterior height.

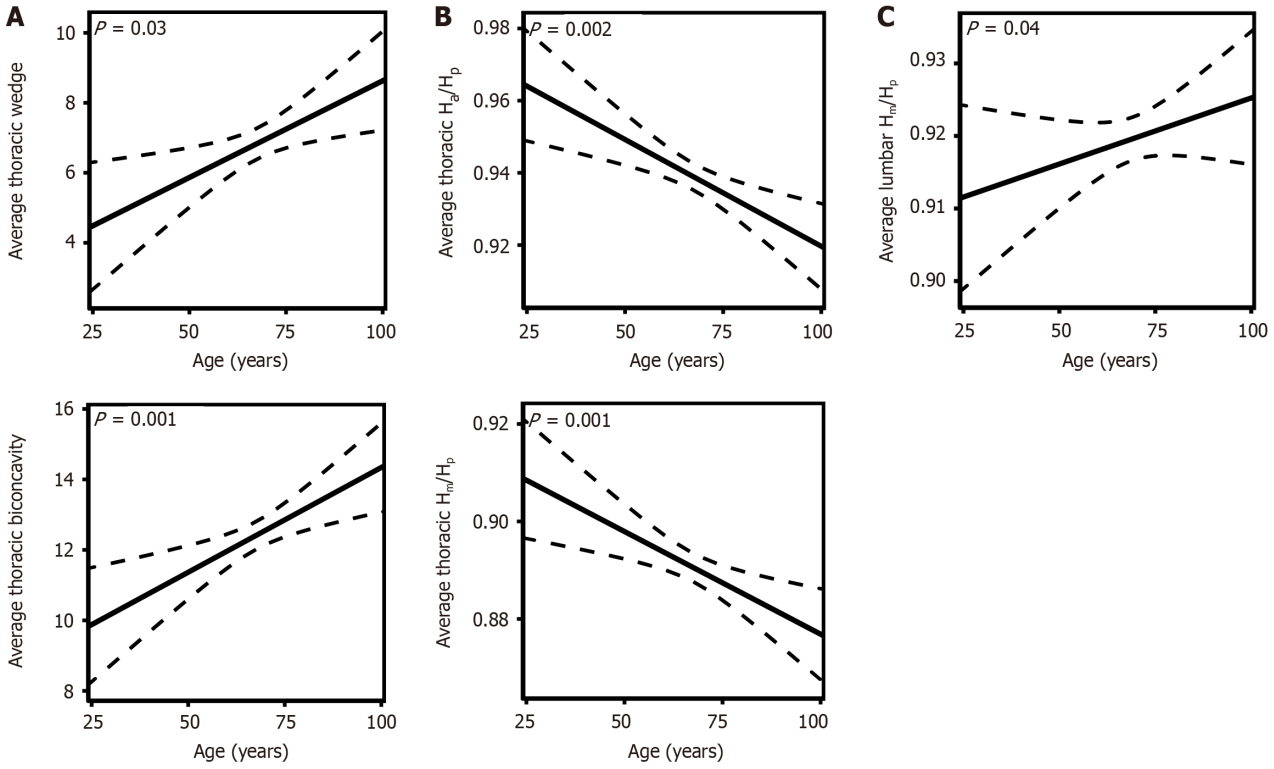

Figure 3 The relationship with age. A: The relationship between age and average thoracic (T1-T12) wedge (left) and biconcavity (right) deformities; B: The relationship between age and average thoracic (T1-T12) anterior height/posterior height (left) and middle height/posterior height (right); C: The relationship between age and average lumbar (L1-L5) middle height/posterior height. H_a: Anterior height; H_m: Middle height; H_p: Posterior height.

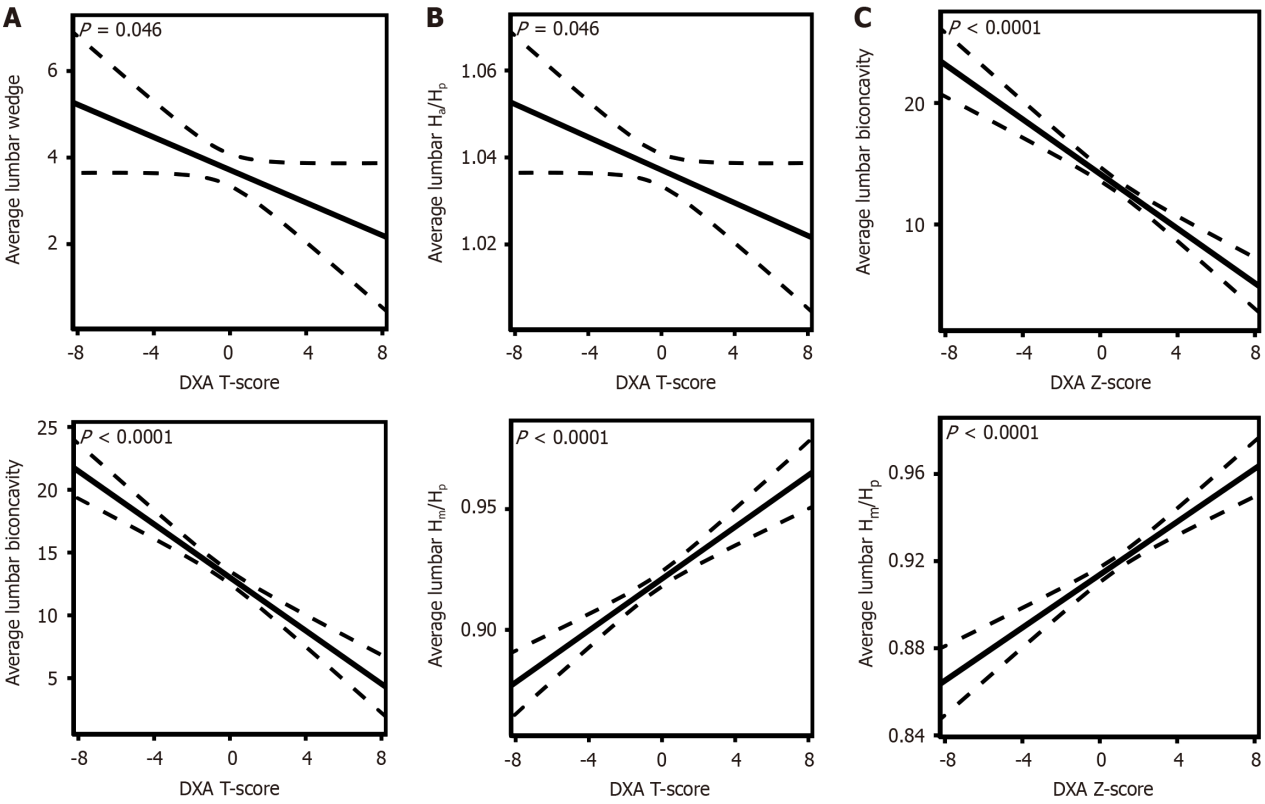

Figure 4 The relationship with dual-energy X-ray absorptiometry scores. A: The relationship between dual-energy X-ray absorptiometry (DXA) T-scores and average lumbar (L1-L5) wedge (left) and biconcavity (right) deformities; B: The relationship between DXA T-scores and average lumbar (L1-L5) anterior height/posterior height (left) and middle height/posterior height (right); C: The relationship between DXA Z-scores and average lumbar (L1-L5) biconcavity (left) and middle height/posterior height (right). DXA: Dual-energy X-ray absorptiometry; H_a: Anterior height; H_m: Middle height; H_p: Posterior height.

(Figure 4B). DXA Z-scores were negatively correlated with lumbar biconcavity (r_s = -0.23, $P < 0.0001$) and H_m/H_p (r_s = 0.18, $P < 0.0001$) (Figure 4C). No significant correlations were identified between DXA T-scores and average lumbar crush or between DXA Z-scores and average lumbar wedge, crush, or H_a/H_p ($P > 0.05$).

MRI cohort compared to 2D existing literature

A qualitative comparison between the MRI cohort and averaged radiograph-derived data from selected prior studies (literature mean) reveals a difference in H_a/H_p by no more than 0.3 at most (Figure 5A), while the maximum difference in H_m/H_p between the two groups is 1.2 (Figure 5B).

DISCUSSION

The primary aims of this study were to establish C3-L5 deformity reference values for a clinically relevant population of females using MR images, to determine the association between deformity severity and age, and to validate MRI-derived reference data against previously published radiograph-derived vertebral heights. As hypothesized, multiple vertebral deformities increased in severity with age. Mean calculations of H_a/H_p and H_m/H_p ratios were comparable between the MRI cohort and the existing radiographic literature. Quantitative analyses were, however, performed within the MRI cohort to compare wedge, crush, biconcavity, H_a/H_p, and H_m/H_p with age and DXA BMD scores. A fixed field of view limited the number of vertebrae we could analyze, so calculations specifically for the C3-C5 vertebrae do not include all participants. Vertebral fracture incidences occur most often at T7-T9 due to thoracic kyphosis and L1-L5 due to activities that increase the axial load[31]. We, therefore, do not believe this omittance will alter the clinical utility of this data.

Additionally, the MRI cohort comprises females with clinically necessitated DXA and MRI scans performed at our institution. The mean age of this cohort is 63.5 years, so the vertebral deformity height values do not represent all adult females equally. Given that vertebral fractures and osteoporosis are most common in postmenopausal women[31,32], with women over 60 experiencing 2-2.5 fold compression fractures compared to those under 60 years old, this distribution is clinically reasonable. However, future studies should emphasize compression fractures in younger individuals as many other variables, such as obesity, can increase the likelihood of vertebral compression fractures[33,34]. Due to our study's large sample size, vertebral height data calculated from these MRI scans likely accurately represents the deformity values of women.

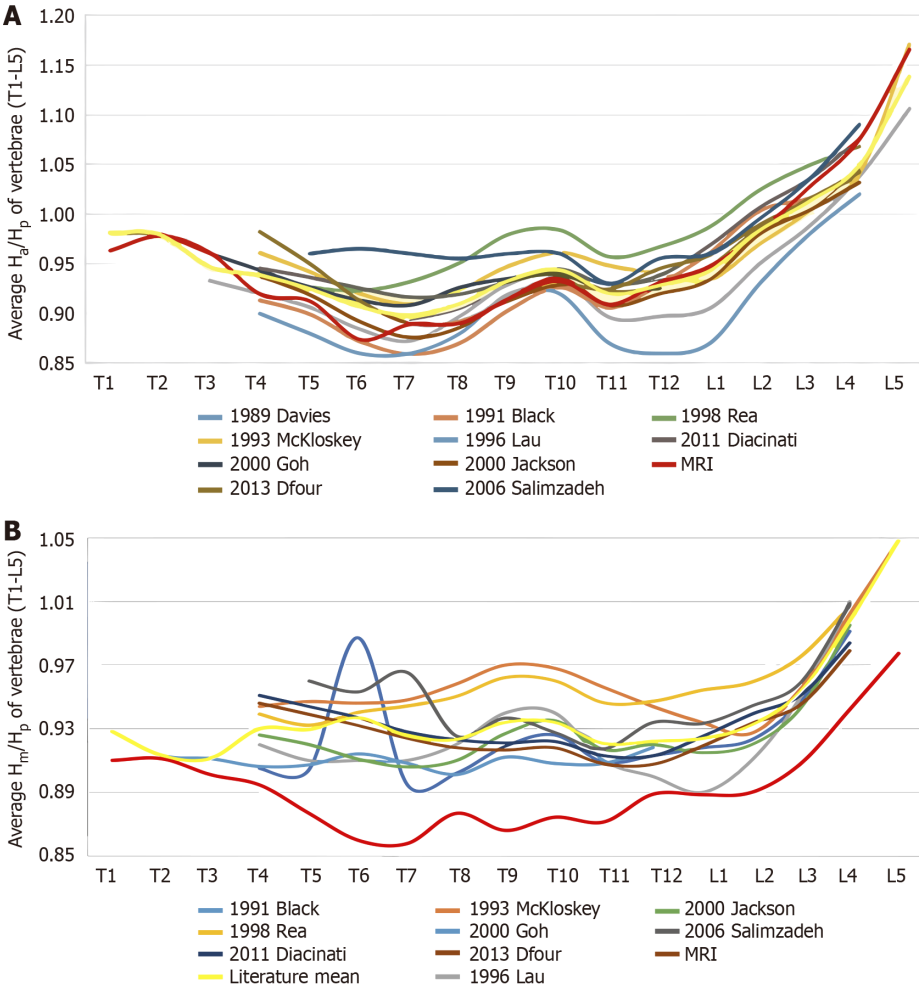

Figure 5 Magnetic resonance imaging cohort compared to two-dimensional existing literature. A: Distribution of average anterior height/posterior height from prior studies. The magnetic resonance imaging cohort (red) differs from the two-dimensional radiograph-derived literature mean (yellow) by a maximum of 0.3; B: Distribution of average middle height/posterior height from prior studies. The magnetic resonance imaging cohort (red) differs from the two-dimensional radiograph-derived literature mean (yellow) by a maximum of 1.2. H_a: Anterior height; H_m: Middle height; H_p: Posterior height.

Comparisons between MRI deformity calculations and DXA T-score and Z-score support the notion that MRI can be used to classify fracture severity of the spine accurately[35,36]. Specifically, lumbar wedge, biconcavity, H_a/H_p, and H_m/H_p correlate with DXA T-scores, and lumbar biconcavity and H_m/H_p correlate with DXA Z-scores. MRI deformity calculation methods should be studied further to replicate our results. Spine and proximal hip BMD provide valuable clinical information, but there is debate about which offers greater predictability of vertebral fracture[35,37,38]. Future comparisons of deformity calculations using MRI with BMD should account for both spine and hip scores. Due to the high contrast possible with MR imaging of soft tissue and bone[39], predictive fracture risk and deformity severity can be determined using manually calculated heights at individual vertebrae instead of DXA, which relies on a broader diagnostic measurement.

Our results also indicate a significant increase in deformity values of lumbar and thoracic biconcavity and H_m/H_p, as well as thoracic wedge and H_a/H_p with age. This observation is supported by the fact that osteoporosis and resultant vertebral fractures are most common in older women[40], which is why age is highlighted as a risk factor for multiple fractures and osteoporosis in studies utilizing radiography[41-45]. Our age-related findings, therefore, validate our MRI-based reference data, further supporting the potential clinical utility of MRI in deformity calculation and assessment. While quantifying vertebral deformities from MRI data has not been widely adopted in routine clinical practice yet, largely due to the labor-intensive nature of these calculations, recent advancements in artificial intelligence-assisted imaging hold great promise. Automation through machine learning algorithms has the potential to streamline these measurements, making MRI a more feasible option for vertebral deformity assessment in clinical settings[46]. Additionally, the use of opportunistic MRI scans provides a unique opportunity to gather valuable clinical data without additional radiation exposure. MRIs conducted for unrelated clinical reasons could be repurposed to automatically assess vertebral deformities, thus allowing for proactive monitoring of spine health. By leveraging these opportunistic MRIs, vertebral deformities could be assessed as an early prognostic marker for fracture risk, particularly in populations prone to osteoporosis and spinal degeneration.

Several limitations should be considered. Although no qualitatively large variation was present, there was no quantitative comparison of the MRI cohort's vertebral heights with previously published vertebral heights. Raw radiographic-derived patient data was not published, which limited our knowledge of variance and distribution[20-30]. Also, it is important to note that consecutive vertebral deformities may introduce inaccuracies in calculating crush deformities since these deformity calculations rely on the above and below vertebrae as reference points. Additionally, further studies are needed to better understand the relationships between vertebral deformity severity and other clinical factors and demographics, such as race, body mass index, weight, height, baseline activity level, comorbidities, and medication usage. Future analyses should focus on stratifying participants by these factors to assess their impact on vertebral deformity progression and severity in women at different stages of life.

CONCLUSION

Clinically, MRI is more expensive and time-consuming than DXA. However, MRI can be advantageous because it does not subject patients to ionizing radiation[47]. With further investigation, MRI has the potential to be used in clinical settings to detect vertebral fractures. We believe opportunistic spinal MRI analysis conducted over a patient's lifetime would allow for prophylactic monitoring of spine health and vertebral deformity progression. Conducting vertebral deformity calculations on routine MRI scans could prove beneficial, as vertebral fractures often go undetected and can have severe ramifications on the quality of life[31]. Additionally, opportunistic analysis would provide more data on vertebral fracture rates in younger individuals. In summary, calculating vertebral deformities using MRI has many benefits, ranging from improving health outcomes to expanding research on MRI's involvement in detecting spine-related diseases.

FOOTNOTES

Author contributions: Sorci OR, Madi R, Kim SM, Batzdorf AS, Alecxih A, Hornyak JN, Patel S, and Rajapakse CS contributed to the design of the research study, performing the research, analyzing the data, and writing the manuscript; and all authors reviewed and edited the final manuscript.

Institutional review board statement: This study was approved by the Institutional Review Board at the University of Pennsylvania (Approval No. 824040).

Informed consent statement: Patients were not required to provide informed consent for this study because the analysis used anonymous clinical data that were obtained after patient had agreed to treatment with written consent.

Conflict-of-interest statement: All the authors report no relevant conflicts of interest for this article.

Data sharing statement: The dataset used and analyzed during the current study is available from the corresponding author at rashad.madi@pennmedicine.upenn.edu upon request.

STROBE statement: The authors have read the STROBE Statement-checklist of items, and the manuscript was prepared and revised according to the STROBE Statement-checklist of items.

Country of origin: United States

ORCID number: Rashad Madi 0000-0002-7498-3244.

S-Editor: Wei YF
L-Editor: A
P-Editor: Wang WB

REFERENCES

1 **Ulivieri FM**, Silva BC, Sardanelli F, Hans D, Bilezikian JP, Caudarella R. Utility of the trabecular bone score (TBS) in secondary osteoporosis. *Endocrine* 2014; **47**: 435-448 [PMID: 24853880 DOI: 10.1007/s12020-014-0280-4]
2 **Wong CC**, McGirt MJ. Vertebral compression fractures: a review of current management and multimodal therapy. *J Multidiscip Healthc* 2013; **6**: 205-214 [PMID: 23818797 DOI: 10.2147/JMDH.S31659]
3 **Tran O**, Silverman S, Xu X, Bonafede M, Fox K, McDermott M, Gandra S. Long-term direct and indirect economic burden associated with

osteoporotic fracture in US postmenopausal women. *Osteoporos Int* 2021; **32**: 1195-1205 [PMID: 33411007 DOI: 10.1007/s00198-020-05769-3]

4 **Salaffi F**, Cimmino MA, Malavolta N, Carotti M, Di Matteo L, Scendoni P, Grassi W; Italian Multicentre Osteoporotic Fracture Study Group. The burden of prevalent fractures on health-related quality of life in postmenopausal women with osteoporosis: the IMOF study. *J Rheumatol* 2007; **34**: 1551-1560 [PMID: 17516618]

5 **Silverman SL**, Minshall ME, Shen W, Harper KD, Xie S; Health-Related Quality of Life Subgroup of the Multiple Outcomes of Raloxifene Evaluation Study. The relationship of health-related quality of life to prevalent and incident vertebral fractures in postmenopausal women with osteoporosis: results from the Multiple Outcomes of Raloxifene Evaluation Study. *Arthritis Rheum* 2001; **44**: 2611-2619 [PMID: 11710717 DOI: 10.1002/1529-0131(200111)44:11<2611::aid-art441>3.0.co;2-n]

6 **Gold DT**. The clinical impact of vertebral fractures: quality of life in women with osteoporosis. *Bone* 1996; **18**: 185S-189S [PMID: 8777086 DOI: 10.1016/8756-3282(95)00500-5]

7 **Szulc P**, Munoz F, Sornay-Rendu E, Paris E, Souhami E, Zanchetta J, Bagur A, van der Mooren MJ, Young S, Delmas PD. Comparison of morphometric assessment of prevalent vertebral deformities in women using different reference data. *Bone* 2000; **27**: 841-846 [PMID: 11113396 DOI: 10.1016/s8756-3282(00)00398-7]

8 **McCarthy J**, Davis A. Diagnosis and Management of Vertebral Compression Fractures. *Am Fam Physician* 2016; **94**: 44-50 [PMID: 27386723]

9 **Berger A**. Bone mineral density scans. *BMJ* 2002; **325**: 484 [PMID: 12202332 DOI: 10.1136/bmj.325.7362.484]

10 **Blake GM**, Fogelman I. The role of DXA bone density scans in the diagnosis and treatment of osteoporosis. *Postgrad Med J* 2007; **83**: 509-517 [PMID: 17675543 DOI: 10.1136/pgmj.2007.057505]

11 **Samelson EJ**, Christiansen BA, Demissie S, Broe KE, Louie-Gao Q, Cupples LA, Roberts BJ, Manoharam R, D'Agostino J, Lang T, Kiel DP, Bouxsein ML. QCT measures of bone strength at the thoracic and lumbar spine: the Framingham Study. *J Bone Miner Res* 2012; **27**: 654-663 [PMID: 22143959 DOI: 10.1002/jbmr.1482]

12 **Genant HK**, Wu CY, van Kuijk C, Nevitt MC. Vertebral fracture assessment using a semiquantitative technique. *J Bone Miner Res* 1993; **8**: 1137-1148 [PMID: 8237484 DOI: 10.1002/jbmr.5650080915]

13 **Moyad MA**. Osteoporosis: a rapid review of risk factors and screening methods. *Urol Oncol* 2003; **21**: 375-379 [PMID: 14670548 DOI: 10.1016/s1078-1439(03)00140-6]

14 **Eastell R**, Cedel SL, Wahner HW, Riggs BL, Melton LJ 3rd. Classification of vertebral fractures. *J Bone Miner Res* 1991; **6**: 207-215 [PMID: 2035348 DOI: 10.1002/jbmr.5650060302]

15 **Rajapakse CS**, Phillips EA, Sun W, Wald MJ, Magland JF, Snyder PJ, Wehrli FW. Vertebral deformities and fractures are associated with MRI and pQCT measures obtained at the distal tibia and radius of postmenopausal women. *Osteoporos Int* 2014; **25**: 973-982 [PMID: 24221453 DOI: 10.1007/s00198-013-2569-1]

16 **Jiang G**, Eastell R, Barrington NA, Ferrar L. Comparison of methods for the visual identification of prevalent vertebral fracture in osteoporosis. *Osteoporos Int* 2004; **15**: 887-896 [PMID: 15071725 DOI: 10.1007/s00198-004-1626-1]

17 **Vrtovec T**, Pernus F, Likar B. A review of methods for quantitative evaluation of spinal curvature. *Eur Spine J* 2009; **18**: 593-607 [PMID: 19247697 DOI: 10.1007/s00586-009-0913-0]

18 **Kallmes DF**, Hui FK, Mugler JP 3rd. Suppression of cerebrospinal fluid and blood flow artifacts in FLAIR MR imaging with a single-slab three-dimensional pulse sequence: initial experience. *Radiology* 2001; **221**: 251-255 [PMID: 11568348 DOI: 10.1148/radiol.2211001712]

19 **Lechner R**, Putzer D, Dammerer D, Liebensteiner M, Bach C, Thaler M. Comparison of two- and three-dimensional measurement of the Cobb angle in scoliosis. *Int Orthop* 2017; **41**: 957-962 [PMID: 27921155 DOI: 10.1007/s00264-016-3359-0]

20 **Davies KM**, Recker RR, Heaney RP. Normal vertebral dimensions and normal variation in serial measurements of vertebrae. *J Bone Miner Res* 1989; **4**: 341-349 [PMID: 2763872 DOI: 10.1002/jbmr.5650040308]

21 **Black DM**, Cummings SR, Stone K, Hudes E, Palermo L, Steiger P. A new approach to defining normal vertebral dimensions. *J Bone Miner Res* 1991; **6**: 883-892 [PMID: 1785377 DOI: 10.1002/jbmr.5650060814]

22 **Ross P**, Wasnich R, Davis J, Vogel J. Vertebral dimension differences between Caucasian populations, and between Caucasians and Japanese. *Bone* 1991; **12**: 107-112 [DOI: 10.1016/8756-3282(91)90008-7]

23 **McCloskey EV**, Spector TD, Eyres KS, Fern ED, O'Rourke N, Vasikaran S, Kanis JA. The assessment of vertebral deformity: a method for use in population studies and clinical trials. *Osteoporos Int* 1993; **3**: 138-147 [PMID: 8481590 DOI: 10.1007/BF01623275]

24 **Lau EM**, Chan HH, Woo J, Lin F, Black D, Nevitt M, Leung PC. Normal ranges for vertebral height ratios and prevalence of vertebral fracture in Hong Kong Chinese: a comparison with American Caucasians. *J Bone Miner Res* 1996; **11**: 1364-1368 [PMID: 8864912 DOI: 10.1002/jbmr.5650110922]

25 **Rea JA**, Steiger P, Blake GM, Potts E, Smith IG, Fogelman I. Morphometric X-ray absorptiometry: reference data for vertebral dimensions. *J Bone Miner Res* 1998; **13**: 464-474 [PMID: 9525347 DOI: 10.1359/jbmr.1998.13.3.464]

26 **Goh S**, Tan C, Price RI, Edmondston SJ, Song S, Davis S, Singer KP. Influence of age and gender on thoracic vertebral body shape and disc degeneration: an MR investigation of 169 cases. *J Anat* 2000; **197** Pt 4: 647-657 [PMID: 11197538 DOI: 10.1046/j.1469-7580.2000.19740647.x]

27 **Jackson SA**, Tenenhouse A, Robertson L. Vertebral fracture definition from population-based data: preliminary results from the Canadian Multicenter Osteoporosis Study (CaMos). *Osteoporos Int* 2000; **11**: 680-687 [PMID: 11095171 DOI: 10.1007/s001980070066]

28 **Diacinti D**, Pisani D, Del Fiacco R, Francucci CM, Fiore CE, Frediani B, Barone A, Bartalena T, Cattaruzza MS, Guglielmi G, Diacinti D, Romagnoli E, Minisola S. Vertebral morphometry by X-ray absorptiometry: which reference data for vertebral heights? *Bone* 2011; **49**: 526-536 [PMID: 21672644 DOI: 10.1016/j.bone.2011.05.027]

29 **Dufour R**, Winzenrieth R, Heraud A, Hans D, Mehsen N. Generation and validation of a normative, age-specific reference curve for lumbar spine trabecular bone score (TBS) in French women. *Osteoporos Int* 2013; **24**: 2837-2846 [PMID: 23681084 DOI: 10.1007/s00198-013-2384-8]

30 **Salimzadeh A**, Moghaddassi M, Alishiri GH, Owlia MB, Kohan L. Vertebral morphometry reference data by X-ray absorptiometry (MXA) in Iranian women. *Clin Rheumatol* 2007; **26**: 704-709 [PMID: 16941205 DOI: 10.1007/s10067-006-0379-y]

31 **Schousboe JT**. Epidemiology of Vertebral Fractures. *J Clin Densitom* 2016; **19**: 8-22 [PMID: 26349789 DOI: 10.1016/j.jocd.2015.08.004]

32 **Kendler DL**, Bauer DC, Davison KS, Dian L, Hanley DA, Harris ST, McClung MR, Miller PD, Schousboe JT, Yuen CK, Lewiecki EM. Vertebral Fractures: Clinical Importance and Management. *Am J Med* 2016; **129**: 221.e1-221.10 [PMID: 26524708 DOI: 10.1016/j.amjmed.2015.09.020]

33 **Bachmann KN**, Bruno AG, Bredella MA, Schorr M, Lawson EA, Gill CM, Singhal V, Meenaghan E, Gerweck AV, Eddy KT, Ebrahimi S, Koman SL, Greenblatt JM, Keane RJ, Weigel T, Dechant E, Misra M, Klibanski A, Bouxsein ML, Miller KK. Vertebral Strength and Estimated Fracture Risk Across the BMI Spectrum in Women. *J Bone Miner Res* 2016; **31**: 281-288 [PMID: 26332401 DOI: 10.1002/jbmr.2697]

34 **Premaor MO**, Comim FV, Compston JE. Obesity and fractures. *Arq Bras Endocrinol Metabol* 2014; **58**: 470-477 [PMID: 25166037 DOI: 10.1590/0004-2730000003274]

35 **O'Gradaigh D**, Debiram I, Love S, Richards HK, Compston JE. A prospective study of discordance in diagnosis of osteoporosis using spine and proximal femur bone densitometry. *Osteoporos Int* 2003; **14**: 13-18 [PMID: 12577180 DOI: 10.1007/s00198-002-1311-1]

36 **Roux C**, Briot K. Current role for bone absorptiometry. *Joint Bone Spine* 2017; **84**: 35-37 [PMID: 27282091 DOI: 10.1016/j.jbspin.2016.02.032]

37 **Schneider DL**, Bettencourt R, Barrett-Connor E. Clinical utility of spine bone density in elderly women. *J Clin Densitom* 2006; **9**: 255-260 [PMID: 16931341 DOI: 10.1016/j.jocd.2006.04.116]

38 **Younes M**, Ben Hammouda S, Jguirim M, Younes K, Zrour S, Béjia I, Touzi M, Bergaoui N. [Discordance between spine and hip Bone Mineral Density measurement using DXA in osteoporosis diagnosis: prevalence and risk factors]. *Tunis Med* 2014; **92**: 1-5 [PMID: 24879162]

39 **Gong H**, Xu S, Xu W, Wang S, Dai X, Qu B. [Acceptance Test and Image Quality Assurance of MRI Simulator Equipment]. *Zhongguo Yi Liao Qi Xie Za Zhi* 2018; **42**: 455-459 [PMID: 30560631 DOI: 10.3969/j.issn.1671-7104.2018.06.019]

40 **Lane NE**. Epidemiology, etiology, and diagnosis of osteoporosis. *Am J Obstet Gynecol* 2006; **194**: S3-11 [PMID: 16448873 DOI: 10.1016/j.ajog.2005.08.047]

41 **Barton DW**, Behrend CJ, Carmouche JJ. Rates of osteoporosis screening and treatment following vertebral fracture. *Spine J* 2019; **19**: 411-417 [PMID: 30142455 DOI: 10.1016/j.spinee.2018.08.004]

42 **Camacho PM**, Petak SM, Binkley N, Clarke BL, Harris ST, Hurley DL, Kleerekoper M, Lewiecki EM, Miller PD, Narula HS, Pessah-Pollack R, Tangpricha V, Wimalawansa SJ, Watts NB. American association of clinical endocrinologists and american college of endocrinology clinical practice guidelines for the diagnosis and treatment of postmenopausal osteoporosis - 2016. *Endocr Pract* 2016; **22**: 1-42 [PMID: 27662240 DOI: 10.4158/EP161435.GL]

43 **Oei L**, Koromani F, Breda SJ, Schousboe JT, Clark EM, van Meurs JB, Ikram MA, Waarsing JH, van Rooij FJ, Zillikens MC, Krestin GP, Oei EH, Rivadeneira F. Osteoporotic Vertebral Fracture Prevalence Varies Widely Between Qualitative and Quantitative Radiological Assessment Methods: The Rotterdam Study. *J Bone Miner Res* 2018; **33**: 560-568 [PMID: 28719143 DOI: 10.1002/jbmr.3220]

44 **Schousboe JT**. Vertebral Fracture Identification as Part of a Comprehensive Risk Assessment in Patients with Osteoporosis. *Curr Osteoporos Rep* 2018; **16**: 573-583 [PMID: 30116975 DOI: 10.1007/s11914-018-0472-6]

45 **Zeytinoglu M**, Jain RK, Vokes TJ. Vertebral fracture assessment: Enhancing the diagnosis, prevention, and treatment of osteoporosis. *Bone* 2017; **104**: 54-65 [PMID: 28285014 DOI: 10.1016/j.bone.2017.03.004]

46 **Suri A**, Jones BC, Ng G, Anabaraonye N, Beyrer P, Domi A, Choi G, Tang S, Terry A, Leichner T, Fathali I, Bastin N, Chesnais H, Taratuta E, Kneeland BJ, Rajapakse CS. Vertebral Deformity Measurements at MRI, CT, and Radiography Using Deep Learning. *Radiol Artif Intell* 2022; **4**: e210015 [PMID: 35146432 DOI: 10.1148/ryai.2021210015]

47 **Chang G**, Boone S, Martel D, Rajapakse CS, Hallyburton RS, Valko M, Honig S, Regatte RR. MRI assessment of bone structure and microarchitecture. *J Magn Reson Imaging* 2017; **46**: 323-337 [PMID: 28165650 DOI: 10.1002/jmri.25647]

Published by **Baishideng Publishing Group Inc**
7041 Koll Center Parkway, Suite 160, Pleasanton, CA 94566, USA
Telephone: +1-925-3991568
E-mail: office@baishideng.com
Help Desk: https://www.f6publishing.com/helpdesk
https://www.wjgnet.com